J|A|C|S
ARTICLES

Published on Web 05/15/2008

Insight into Substrate Binding in Shibasaki's $Li_3(THF)_n(BINOLate)_3Ln$ Complexes and Implications in Catalysis

Alfred J. Wooten, Patrick J. Carroll, and Patrick J. Walsh*

P. Roy and Diana T. Vagelos Laboratories, Department of Chemistry, University of Pennsylvania, 231 South 34th Street, Philadelphia, Pennsylvania 19104-6323

Received December 7, 2007; E-mail: pwalsh@sas.upenn.edu

Abstract: Heterobimetallic Lewis acids $M_3(THF)_n(BINOLate)_3Ln$ [M = Li, Na, K; Ln = lanthanide(III)] are exceptionally useful asymmetric catalysts that exhibit high levels of enantioselectivity across a wide range of reactions. Despite their prominence, important questions remain regarding the nature of the catalyst−substrate interactions and, therefore, the mechanism of catalyst operation. Reported herein are the isolation and structural characterization of 7- and 8-coordinate heterobimetallic complexes $Li_3(THF)_4(BINOLate)_3Ln(THF)$ [Ln = La, Pr, and Eu], $Li_3(py)_5(BINOLate)_3Ln(py)$ [Ln = Eu and Yb], and $Li_3(py)_5(BINOLate)_3La(py)_2$ [py = pyridine]. Solution binding studies of cyclohexenone, DMF, and pyridine with $Li_3(THF)_n(BINOLate)_3Ln$ [Ln = Eu, Pr, and Yb] and $Li_3(DMEDA)_3(BINOLate)_3Ln$ [Ln = La and Eu; DMEDA = *N,N*′-dimethylethylene diamine] demonstrate binding of these Lewis basic substrate analogues to the lanthanide center. The paramagnetic europium, ytterbium, and praseodymium complexes $Li_3(THF)_n(BINOLate)_3Ln$ induce relatively large lanthanide-induced shifts on substrate analogues that ranged from 0.5 to 4.3 ppm in the ^1H NMR spectrum. X-ray structure analysis and NMR studies of $Li_3(DMEDA)_3(BINOLate)_3Ln$ [Ln = Lu, Eu, La, and the transition metal analogue Y] reveal selective binding of DMEDA to the lithium centers. Upon coordination of DMEDA, six new stereogenic nitrogen centers are formed with perfect diastereoselectivity in the solid state, and only a single diastereomer is observed in solution. The lithium-bound DMEDA ligands are not displaced by cyclohexenone, DMF, or THF on the NMR time scale. Use of the DMEDA adduct $Li_3(DMEDA)_3(BINOLate)_3La$ in three catalytic asymmetric reactions led to enantioselectivities similar to those obtained with Shibasaki's $Li_3(THF)_n(BINOLate)_3La$ complex. Also reported is a unique dimeric $[Li_6(en)_7(BINOLate)_6Eu_2][\mu\text{-}\eta^1,\eta^1\text{-en}]$ structure [en = ethylenediamine]. On the basis of these studies, it is hypothesized that the lanthanide in Shibasaki's $Li_3(THF)_n(BINOLate)_3Ln$ complexes cannot bind bidentate substrates in a chelating fashion. A hypothesis is also presented to explain why the lanthanide catalyst, $Li_3(THF)_n(BINOLate)_3La$, is often the most enantioselective of the $Li_3(THF)_n(BINOLate)_3Ln$ derivatives.

1. Introduction

The development and application of bifunctional catalysts for use in asymmetric catalysis continues to gain importance.[1–10] The unique features of these catalysts that enable their cooperative reactivity also open new reaction manifolds. Understanding how bifunctional catalysts operate is imperative to the rational development of improved and innovative catalysts. The very characteristics that are responsible for the multifunctional nature of these catalysts, however, often complicate mechanistic studies.

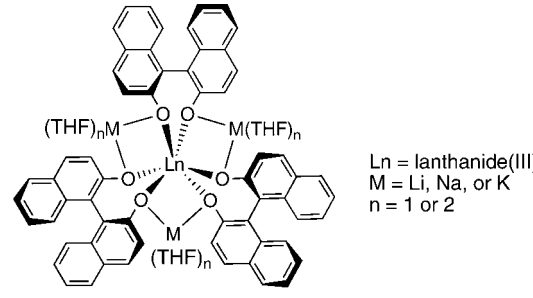

Figure 1. Shibasaki's $M_3(THF)_n(BINOLate)_3Ln$ catalysts.

Perhaps the most prominent class of multifunctional enantioselective catalysts is Shibasaki's heterobimetallic complexes, $M_3(THF)_n(BINOLate)_3Ln$ (Figure 1), which contain Lewis acidic lanthanide(III) and main group (M = Li, Na, K) metals in addition to the Lewis and Brønsted basic oxygens of the

(1) Kanai, M.; Kato, N.; Ichikawa, E.; Shibasaki, M. *Synlett* **2005**, 1491–1508.
(2) Ma, J.-A.; Cahard, D. *Angew. Chem., Int. Ed.* **2004**, *43*, 4566–4583.
(3) Rowlands, G. J. *Tetrahedron* **2001**, *57*, 1865–1882.
(4) van den Beuken, E. K.; Feringa, B. L. *Tetrahedron* **1998**, *54*, 12985–13011.
(5) Sawamura, M.; Ito, Y. *Chem. Rev.* **1992**, *92*, 857–871.
(6) Shibasaki, M.; Yoshikawa, N. *Chem. Rev.* **2002**, *102*, 2187–2219.
(7) Shibasaki, M.; Kanai, M.; Funabashi, K. *J. Chem. Soc., Chem. Commun.* **2002**, 1989–1999.
(8) Noyori, R.; Yamakawa, M.; Hashiguchi, S. *J. Org. Chem.* **2001**, *66*, 7931–7944.
(9) Noyori, R.; Ohkuma, T. *Angew. Chem., Int. Ed.* **2001**, *40*, 40–73.
(10) Noyori, R.; Hashiguchi, S. *Acc. Chem. Res.* **1997**, *30*, 97–102.

BINOLate ligands.[11,7,6] They have been successfully employed in many asymmetric reactions, including the Henry reaction,[11,12] nucleophilic conjugate additions,[12–15] the aldol reaction,[16,17] the cyano-ethoxycarbonylation reaction,[18] the asymmetric 1,4-addition of *O*-alkylhydroxylamine to enones,[19] and the phosphonylation of aldehydes,[20] to name a few.

Key to the success of Shibasaki's heterobimetallic $M_3(THF)_n$-$(BINOLate)_3Ln$ catalysts is the tunability of their chiral environment. In moving from left to right across the lanthanide series, the lanthanide contraction causes a decrease in the ionic radii from 1.17 Å for lanthanum to 1.00 Å for lutetium.[21–23] As a result, each isostructural lanthanide complex $M_3(THF)_n$-$(BINOLate)_3Ln$ will exhibit different activity and enantioselectivity.[24] Furthermore, the alkali metal ionic radius can also be varied from 1.52 (K^+) to 1.16 (Na^+) and 0.90 Å (Li^+),[25] providing three sets of $M_3(THF)_n(BINOLate)_3Ln$ catalysts that usually exhibit very different catalytic behavior.

Despite the widespread application of Shibasaki's catalysts, fundamental questions remain concerning substrate binding: To which metal does the substrate bind? Can bidentate substrates chelate to these complexes? Although most reactions have been proposed to involve substrate activation by the lanthanide center,[7,6,19,26,27] it has been suggested that the Diels–Alder reaction[28] and the cyano-ethoxycarbonylation of aldehydes[18] involve substrate activation by the alkali metals (lithium).

Investigations into Shibasaki's catalysts by other groups focused on their solid-state structures. The structures of several 6-coordinate $M_3(sol)_n(BINOLate)_3Ln$ (Figure 1)[29,30] and 7-coordinate $M_3(sol)_n(BINOLate)_3Ln(OH_2)$[11,15,29,31] [sol = THF or Et_2O; M = Li or Na] lanthanide complexes have been reported.[32] The lanthanides in these structures are bound to the six BINOLate oxygens, and in some cases, they also bind a water molecule. Curiously, despite crystallization from Lewis basic solvents such as THF and diethyl ether, no lanthanide solvates had been characterized crystallographically prior to the studies outlined herein. In contrast, the alkali metals are always bound to one or two solvent molecules [THF or Et_2O] in the solid state. Furthermore, Salvadori and co-workers demonstrated that the Yb center in $M_3(THF)_n(BINOLate)_3Yb$ complexes [M = Na and K] does not even bind water in solution or the solid state. The reluctance of the ytterbium center to coordinate water was attributed to its ionic radius (1.01 Å), which is among the shortest in the lanthanide series.[30,33]

The absence of structurally characterized $M_3(sol)_n(BINOLate)_3Ln(S)_x$ complexes [M = Li, Na, or K; S = substrate or solvent] with lanthanide-bound organic Lewis bases, and the experimental evidence suggesting that the alkali metals (lithium) are catalytically active in some reactions,[18,28] led us to wonder if perhaps the main group metals were responsible for the observed substrate activation with these catalysts and if the lanthanide was only a structural element. Solution NMR studies are generally useful to probe substrate binding to metal complexes. In the case of bimetallic $M_3(sol)_n(BINOLate)_3Ln$ complexes, however, distinguishing binding at the lanthanide from binding at the main group metals is not trivial.

To better understand $M_3(sol)_n(BINOLate)_3Ln$ complexes, and to aid in the design of related catalysts, we initiated studies to determine if the lanthanide centers in $Li_3(sol)_n(BINOLate)_3Ln$ complexes are able to bind organic substrates and substrate analogues. Herein we report the full results of our investigations. Our studies indicate that the lanthanides in $Li_3(sol)_n(BINOLate)_3Ln$ complexes, *including Ln = Yb*, can coordinate organic Lewis bases both in the solid state and in solution. We also describe the first structure of an 8-coordinate $M_3(sol)_n(BINOLate)_3Ln(S)_2$ complex and propose an explanation for why $Li_3(sol)_n(BINOLate)_3La$ is usually the most enantioselective of this class of catalysts.[6] Finally, on the basis of these studies, we hypothesize that $Li_3(sol)_n(BINOLate)_3Ln$ catalysts have two pseudo-*trans* binding sites and that chelation of bidentate substrates to the lanthanide is unfavorable. Parts of this work have appeared in preliminary communications.[34–36]

2. Results and Discussion

2.1. Synthesis and Solid-State Structures of 6-, 7-, and 8-Coordinate $Li_3(sol)_n(BINOLate)_3Ln(sol)_x$ Complexes. In this section, we evaluate the capability of $Li_3(sol)_n(BINOLate)_3Ln$ (**1-Ln**) to bind organic Lewis bases at the lanthanide in the solid state. A list of compound abbreviations used in this paper is presented in Table 1.

When we initiated our solid-state structural studies of $M_3(sol)_n(BINOLate)_3Ln$ complexes, there were no examples of characterized $M_3(sol)_n(BINOLate)_3Ln(S)$ complexes (where S is an organic solvent or substrate). To explore binding of substrate analogues to the lanthanide centers in the solid state,

(11) Sasai, H.; Suzuki, T.; Itoh, N.; Tanaka, K.; Date, T.; Okamura, K.; Shibasaki, M. *J. Am. Chem. Soc.* **1993**, *115*, 10372–10373.
(12) Shibasaki, M.; Sasai, H. *Pure Appl. Chem.* **1996**, *68*, 523–530.
(13) Emori, E.; Aria, T.; Sasai, H.; Shibasaki, M. *J. Am. Chem. Soc.* **1998**, *120*, 4043–4044.
(14) Funabashi, K.; Saida, Y.; Kanai, m.; Arai, T.; Sasai, H.; Shibasaki, M. *Tetrahedron Lett.* **1998**, *39*, 7557–7558.
(15) Sasai, H.; Arai, T.; Satow, Y.; Houk, K. N.; Shibasaki, M. *J. Am. Chem. Soc.* **1995**, *117*, 6194–6198.
(16) Yamada, Y. M. A.; Yoshikawa, N.; Sasai, H.; Shibasaki, M. *Angew. Chem., Int. Ed.* **1997**, *36*, 1871–1873.
(17) Yoshikawa, N.; Kumagai, N.; Matsunaga, S.; Moll, G.; Ohshima, T.; Suzuki, T.; Shibasaki, M. *J. Am. Chem. Soc.* **2001**, *123*, 2466–2467.
(18) Yamagiwa, N.; Tian, J.; Matsunaga, S.; Shibasaki, M. *J. Am. Chem. Soc.* **2005**, *127*, 3413–3422.
(19) Yamagiwa, N.; Matsunaga, S.; Shibasaki, M. *J. Am. Chem. Soc.* **2003**, *125*, 16178–16179.
(20) Sasai, H.; Bougauchi, M.; Arai, T.; Shibasaki, M. *Tetrahedron Lett.* **1997**, *38*, 2717–2720.
(21) Mikami, K.; Terada, M.; Matsuzawa, H. *Angew. Chem., Int. Ed.* **2002**, *41*, 3555–3571.
(22) Herrmann, W. G., Ed. *Organolanthanoid Chemistry: Synthesis, Structure, Catalysis*; Springer: Berlin, 1996.
(23) Sinha, S. P. *Structures and Bonding*; Springer-Verlag: New York, 1976; Vol. 25.
(24) Yamagiwa, N.; Qiin, H.; Matsunaga, M.; Shibasaki, M. *J. Am. Chem. Soc.* **2005**, *127*, 13419–13427.
(25) Wulfsberg, G. *Principles of Descriptive Inorganic Chemistry*; Brooks/Cole Publishing Co: Monterey, CA, 1987.
(26) Yamagiwa, N.; Matsunaga, S.; Shibasaki, M. *Angew. Chem., Int. Ed.* **2004**, *43*, 4493–4497.
(27) Sasai, H.; Arai, T.; Shibasaki, M. *Angew. Chem., Int. Ed.* **1997**, *36*, 1236–1256.
(28) Morita, T.; Arai, T.; Sasai, H.; Shibasaki, M. *Tetrahedron: Asymmetry* **1998**, *9*, 1445–1450.
(29) Aspinall, H. C.; Bickley, J. F.; Dwyer, J. L. M.; Greeves, N.; Kelly, R. V.; Steiner, A. *Organometallics* **2000**, *19*, 5416–5423.
(30) Di Bari, L.; Lelli, M.; Pintacuda, G.; Pescitelli, G.; Marchetti, F.; Salvadori, P. *J. Am. Chem. Soc.* **2003**, *125*, 5549–5558.
(31) Takaoka, E.; Yoshikawa, N.; Yamada, Y. M. A.; Sasai, H.; Shibasaki, M. *Heterocycles* **1997**, *46*, 157–163.
(32) Aspinall, H. C. *Chem. Rev.* **2002**, *102*, 1807–1850.
(33) Di Bari, L.; Lelli, M.; Salvadori, P. *Chem. Eur. J.* **2004**, *10*, 4594–4598.
(34) Wooten, A. J.; Carroll, P. J.; Walsh, P. J. *Angew. Chem., Int. Ed.* **2006**, *45*, 2549–2552.
(35) Wooten, A. J.; Carroll, P. J.; Walsh, P. J. *Org. Lett.* **2007**, *9*, 3359–3362.
(36) Wooten, A. J.; Salvi, L.; Carroll, P. J.; Walsh, P. J. *Adv. Synth. Catal.* **2007**, *349*, 561–565.

Table 1. Compound Abbreviations

abbreviation	compound
1-Ln	$Li_3(sol)_n(BINOLate)_3Ln$
2-Ln	$Li_3(THF)_4(BINOLate)_3Ln(THF)$, Ln = La, Pr, Eu
3-La	$Li_3(py)_5(BINOLate)_3La(py)_2$
4-Ln	$Li_3(py)_5(BINOLate)_3Ln(py)$, Ln = Eu, Yb
5-Ln	$Li_3(DMEDA)_3(BINOLate)_3Ln$, Ln = La, Eu, Lu, Y
6-Eu	$[Li_6(en)_7(BINOLate)_6Eu_2][\mu\text{-}\eta^1,\eta^1\text{-en}]$

we crystallized Shibasaki's $Li_3(THF)_n(BINOLate)_3Ln$ complexes[11,15,29] [**1-La**, **1-Pr**, **1-Eu**, and **1-Yb**] from anhydrous THF by diffusion of pentane vapor into the solution of the lanthanide complex. The crystals that formed were subject to X-ray analysis and determined to be the isostructural 7-coordinate THF adducts, $Li_3(THF)_4(BINOLate)_3Ln(THF)$ (**2-La**, **2-Pr**, and **2-Eu**).[34] The structure of the praseodymium derivative is illustrated in Figure 2. The gross structural features of the 7-coordinate THF adducts **2-Ln** consist of LnO_7 cores that can be described as trigonally compressed capped octahedrons with THF as the capping group. In contrast, the smaller ytterbium complex crystallized as the 6-coordinate **1-Yb** (Figure 3). Selected bond distances for these compounds are compiled in Table 2. On the basis of Salvadori's solution studies of $M_3(THF)_6(BINOLate)_3Yb$ (M = Na, K),[30] the lower coordination number of the ytterbium derivative might not be surprising. Inspection of the distances in Table 2 indicates that the Ln−O distances of the BINOLate and the THF ligands decrease in the order La > Pr > Eu, as predicted on the basis of decreasing ionic radii. Likewise, the degree of displacement of the central Ln from the Li_3 plane also decreases. Although the ytterbium in **1-Yb** does not bind a THF, the lithium centers bind a total of six THF ligands in the solid state, compared to only four for the 7-coordinate THF adducts (**2-La**, **2-Pr**, and **2-Eu**). We interpret the different number of lithium·THF interactions as a tradeoff between bonding at the lanthanide vs the lithium centers.

To probe binding of softer and smaller pyridine to the lanthanide centers in **1-Ln** (Ln = La, Eu, Yb),[11,15,29] these compounds were dissolved in anhydrous pyridine at room temperature. Pentane vapor was diffused into each pyridine solution to afford pale crystals. The structures were determined at low temperature, and an ORTEP diagram of the lanthanum complex (**3-La**) is illustrated in Figure 4, with relevant bond distances listed in Table 2. $Li_3(py)_5(BINOLate)_3La(py)_2$ (**3-La**) represents the first 8-coordinate derivative of Shibasaki's catalysts.[34] The two pseudo-*trans* pyridine ligands exhibit a N−La−N bond angle of 150.87(8)° and La−N distances of 2.812(3) (La1−N6) and 2.773(3) Å (La1−N7). The BINOLate La−O distances range from 2.439(2) to 2.536(2) Å and are, on average, longer than the BINOLate La−O distances in the 7-coordinate THF adduct **2-La**.[29,34]

On the basis of Salvadori's observation that $Na_3(THF)_6(BINOLate)_3Yb$ does not bind water,[30] and for the purpose of comparison with 8-coordinate **3-La**, complexes **1-Eu** and **1-Yb** were crystallized from pyridine in a fashion similar to **3-La**; their structures were determined at low temperature. ORTEP diagrams of 7-coordinate $Li_3(py)_5(BINOLate)_3Ln(py)$ (**4-Eu**) and (**4-Yb**) are shown in Figures 5 and 6, with selected bond distances in Table 2 (entries 6 and 7).

Like the THF adducts $Li_3(THF)_4(BINOLate)_3Ln(THF)$ (**2-Ln**), the isostructural 7-coordinate pyridine adducts **4-Eu** and **4-Yb** contain trigonally compressed capped octahedral LnO_6N cores with pyridine as the capping ligand. As observed with other $M_3(THF)_n(BINOLate)_3Ln$ complexes,[32] use of (*R*)-BINOL

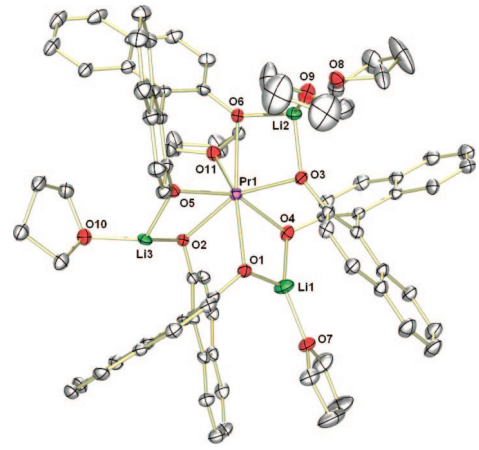

Figure 2. ORTEP of $Li_3(THF)_4(BINOLate)_3Pr(THF)$ (**2-Pr**) with 30% probability thermal ellipsoids.

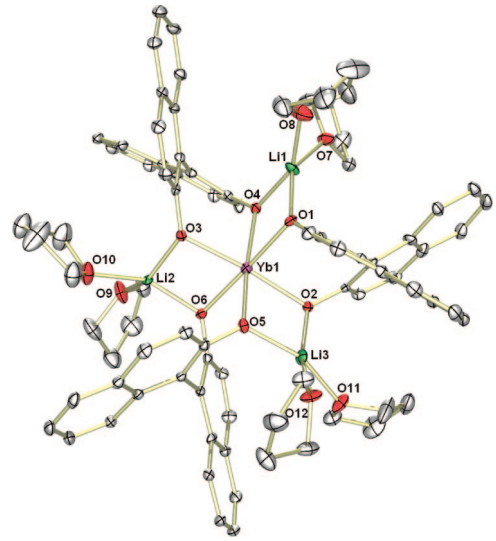

Figure 3. ORTEP of $Li_3(THF)_6(BINOLate)_3Yb$ (**1-Yb**) with 30% probability thermal ellipsoids.

leads to the Δ-configuration at the lanthanide center. Differences in bond distances of **3-La**, **4-Eu**, and **4-Yb** are primarily due to the decreasing ionic radii [La (1.17 Å) to Eu (1.09 Å) and Yb (1.01 Å)]. The Ln−py distances for **4-Eu** [2.578(5) Å] and **4-Yb** [2.470(5) Å] are also shorter than the distances in **3-La** [2.812(3) and 2.773(3) Å]. Pyridine coordination in **4-Eu** causes a 0.4901(2) Å displacement of Eu from the Li_3 plane. The smaller Yb center is displaced by 0.4787(2) Å in **4-Yb**. These displacements are notably smaller than observed in the THF adducts **2-Ln** [La = 0.767(4), Pr = 0.7490(3), and Eu = 0.737(3) Å]. The greater displacement of the lanthanide center in the THF adducts **2-Ln** is consistent with increased size of THF with respect to pyridine. The THF ligands must be further removed from the BINOLates to reduce steric interactions between these ligands. In sharp contrast to displacements from the Li_3 plane in the 7-coordinate THF (**2-Ln**) and pyridine (**4-Ln**) adducts, the La in 8-coordinate **3-La** is displaced by only 0.042 (2) Å.

The results of our crystallographic study, described above, have three important implications concerning substrate binding and catalytic asymmetric reactions with **1-Ln** complexes. First, in contrast to $M_3(sol)_n(BINOLate)_3Yb$ (M = Na, K) catalysts,

Table 2. Selected Bond Distances (Å) and Li_3−Ln Displacement for $Li_3(THF)_6(BINOLate)_3Yb$ (**1-Yb**), THF Adducts $Li_3(THF)_4(BINOLate)_3Ln\cdot THF$ (**2-Eu**, **2-Pr**, and, **2-La**), and Pyridine Adducts $Li_3(py)_5(BINOLate)_3La(py)_2$ (**3-La**) and $Li_3(py)_5(BINOLate)_3Ln(py)$ (**4-Yb** and **4-Eu**)

entry	compound	Ln−$O_{BINOLate}$ (Å)	Ln−O_{THF} (Å)	Ln−N_{Py} (Å)	Li_3−Ln (Å) displacement
1	$Li_3(THF)_6(BINOLate)_3Yb$ (**1-Yb**)	Yb1−O1, 2.203(4) Yb1−O2, 2.200(4) Yb1−O3, 2.210(4) Yb1−O4, 2.205(4) Yb1−O5, 2.214(4) Yb1−O6, 2.207(4)	−	−	0.11246(9)
2	$Li_3(THF)_4(BINOLate)_3Eu(THF)$ (**2-Eu**)	Eu1−O1, 2.400(4) Eu1−O2, 2.385(3) Eu1−O3, 2.302(3) Eu1−O4, 2.364(4) Eu1−O5, 2.302(4) Eu1−O6, 2.379(3)	2.482(4)	−	0.737(3)
3	$Li_3(THF)_4(BINOLate)_3Pr(THF)$ (**2-Pr**)	Pr1−O1, 2.438(4) Pr1−O2, 2.435(3) Pr1−O3, 2.352(3) Pr1−O4, 2.407(4) Pr1−O5, 2.355(4) Pr1−O6, 2.427(3)	2.542(4)	−	0.7490(3)
4	$Li_3(THF)_4(BINOLate)_3La(THF)$ (**2-La**)	La1−O1, 2.473(4) La1−O2, 2.485(3) La1−O3, 2.410(3) La1−O4, 2.449(5) La1−O5, 2.403(5) La1−O6, 2.461(3)	2.567(5)	−	0.767(4)
5	$Li_3(py)_5(BINOLate)_3La(py)_2$ (**3-La**)	La1−O1, 2.514(2) La1−O2, 2.492(2) La1−O3, 2.511(2) La1−O4, 2.536(2) La1−O5, 2.439(2) La1−O6, 2.476(2)	−	2.812(3) 2.773(3)	0.042(2)
6	$Li_3(py)_5(BINOLate)_3Yb(py)$ (**4-Yb**)	Yb1−O1, 2.251(4) Yb1−O2, 2.324(4) Yb1−O3, 2.238(4) Yb1−O4, 2.284(4) Yb1−O5, 2.250(4) Yb1−O6, 2.279(4)	−	2.470(5)	0.4787(2)
7	$Li_3(py)_5(BINOLate)_3Eu(py)$ (**4-Eu**)	Eu1−O1, 2.333(3) Eu1−O2, 2.397(3) Eu1−O3, 2.320(3) Eu1−O4, 2.364(3) Eu1−O5, 2.320(3) Eu1−O6, 2.374(3)	−	2.578(5)	0.4901(2)

which do not bind water in solution or in the solid state,[30] **4-Yb** is capable of binding Lewis bases in the solid state. In section 2.4, evidence will be presented that **1-Yb** can also bind substrate analogues in solution at the lanthanide.

Second, it is often found that the lanthanum derivative $Li_3(THF)_n(BINOLate)_3La$ (**1-La**) is the most enantioselective of the **1-Ln** catalysts. We hypothesize that this may be due to the larger ionic radius of lanthanum, which allows **1-La** to achieve a coordination number of 8. Bonding of two ligands in a pseudo-*trans* fashion to the lanthanum, as observed in the solid-state structure of **3-La**, places the lanthanum in the Li_3 plane. Thus, in an 8-coordinate complex, the lanthanide and substrate are held closer to the chiral environment of the BINOLate ligands than in 7-coordinate complexes, where the lanthanide and the substrate are displaced from the BINOLate ligands (Table 2).

Finally, the observed pseudo-*trans* coordination of pyridines to the lanthanum center in **3-La** led us to question whether the lanthanide in these complexes is capable of binding ligands in a *cis* fashion, as would be necessary to chelate a bidentate substrate. Determination of how substrates coordinate to catalysts is crucial to understanding reaction mechanisms and to rational catalyst optimization. Studies to probe the ability of **1-Ln** complexes to chelate bidentate substrates are outlined in sections 2.5 and 2.7.

2.2. Synthesis and Solid-State Structures of $Li_3(DMEDA)_3(BINOLate)_3Ln$ Complexes. Solution studies of $Li_3(THF)_n(BINOLate)_3Ln$ complexes to detect lanthanide−Lewis base interactions are complicated by the presence of the Lewis acidic lithium centers. The aim of this section is to identify a ligand that will selectively bind to the lithiums of **1-Ln** complexes and enable us to study Ln−Lewis base interactions. Due to the high affinity of lithium for diamines,[37] we screened several

(37) Rutherford, J. L.; Hoffmann, D.; Collum, D. B. *J. Am. Chem. Soc.* **2002**, *124*, 264–271.

diamines and found that *N*,*N*′-dimethylethylene diamine (DMEDA) readily binds to the lithium centers.

Two syntheses of $Li_3(DMEDA)_3(BINOLate)_3Ln$ complexes (**5-Ln**) and the transition metal analogue **5-Y** are outlined in eqs 1 and 2. Addition of 3.3 equiv of DMEDA to **1-Eu** and **1-La**[11,15] in THF resulted in the formation of **5-Eu** and **5-La**.[34] Importantly, DMEDA displaced the THF ligands in **1-Ln** *even in THF solvent*, indicating that the lithium centers have a high affinity for DMEDA. The DMEDA adducts **5-Ln** can be directly synthesized by combining 3 equiv of $(BINOLate)Li_2$, 3.3 equiv of DMEDA, and 1 equiv of $Ln(OSO_2CF_3)_3$ (Ln = Lu, Eu, La, and Y) in THF (eq 2).

$$Li_3(THF)_n(BINOLate)_3Ln + 3.3DMEDA \xrightarrow[rt]{THF} Li_3(DMEDA)_3(BINOLate)_3Ln \quad (1)$$

5-Eu, 85% yield
5-La, 91% yield

$$Ln(OSO_2CF_3)_3 + 3Li_2(BINOLate) + 3.3DMEDA \xrightarrow[rt]{THF} Li_3(DMEDA)_3(BINOLate)_3Ln \quad (2)$$

5-Lu, 63% yield
5-Eu, 61% yield
5-La, 73% yield
5-Y, 67% yield

X-ray-quality crystals of **5-Ln** were obtained by gas-phase diffusion of pentane into a THF solution of each complex at room temperature. X-ray structural studies indicated that **5-Lu**, **5-Eu**, **5-La**, and **5-Y** are isostructural. An ORTEP of **5-Eu** is illustrated in Figure 7, with ORTEPs of **5-Lu**, **5-La**, and **5-Y** in the Supporting Information. Selected bond distances for **5-Lu**, **5-Eu**, **5-La**, and **5-Y** are listed in Table 3. The structures of **5-Ln** consist of 6-coordinate distorted octahedral lanthanide centers, where each lithium is chelated by DMEDA. The Ln−O distances in **5-Eu** and **5-La** are shorter than in the higher coordinate pyridine adducts **4-Eu** and **3-La** (Table 2). The Li−N distances are similar and fall within the range of 2.034(11)−2.138(11) Å.

In general, upon coordination of DMEDA to metals, the nitrogens become stereogenic centers and can adopt the (*R*,*R*)-, (*S*,*S*)-, or (*R*,*S*)-configuration. In the formation of **5-Ln** complexes, this could lead to the generation of many diastereomers. The presence of the (*R*)-BINOLate ligands, however, efficiently biases the stereochemistry of the DMEDA nitrogens such that *six new stereocenters are formed with perfect diastereoselectivity in the solid state*. When (*R*)-BINOL was used in the synthesis of the DMEDA adducts, each nitrogen adopted the (*S*)-configuration, directing the N−H bonds toward the closest naphthyl ring and orienting the *N*-methyl groups away to avoid unfavorable steric interactions (Figure 8). Resonances attributed to a single complex were also observed by solution ^1H and $^{13}C\{^1H\}$ NMR spectroscopy for **5-Lu**, **5-Eu**, **5-La**, and **5-Y** (see section 2.3 and the Supporting Information). Having found a ligand for lithium that inhibits coordination of substrates to these centers, we were positioned to probe binding of the lanthanide in solution.

2.3. Solution NMR Studies of 1-Ln and 5-Ln Complexes. In this section, the NMR properties of paramagnetic heterobimetallic complexes are discussed and compared to those of their diamagnetic counterparts. As outlined in this and the following sections, the paramagnetic properties of Eu, Yb, and Pr were indispensable to these studies.

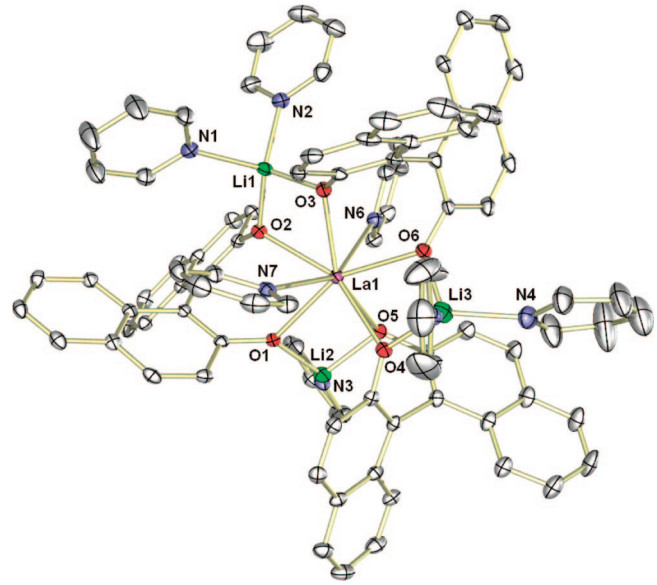

Figure 4. ORTEP of $Li_3(py)_5(BINOLate)_3La(py)_2$ (**3-La**) with 30% probability thermal ellipsoids.

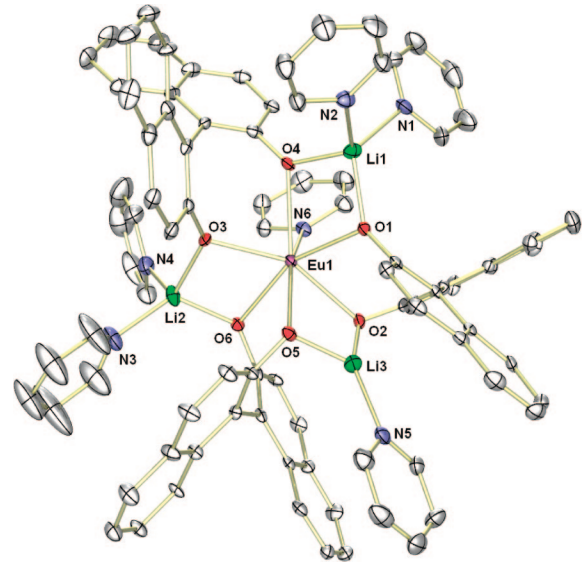

Figure 5. ORTEP of $Li_3(py)_5(BINOLate)_3Eu(py)$ (**4-Eu**) with 30% probability thermal ellipsoids.

NMR binding studies with asymmetric Lewis acid catalysts are often challenging, because the chemical shift changes upon substrate binding to the Lewis acid are often small due to low binding affinities.[38–41] Fortunately, several paramagnetic lanthanide centers are well behaved and are commonly used as NMR shift reagents. The lanthanide-induced shifts (LISs) of ligand protons are very sensitive to perturbations in the coordination environment of paramagnetic lanthanide centers.[38–41] The direction and magnitude of the LIS is dependent on the geometrical factor $(3\cos^2\theta - 1)/r^3$ and the anisotropic *g*-

(38) Cockerill, A. F.; Davies, G. L. O.; Harden, R. C.; Rackham, D. M. *Chem. Rev.* **1973**, *73*, 553–588.
(39) Horrocks, W. D.; Sipe, J. P. *J. Am. Chem. Soc.* **1971**, *93*, 6800–6804.
(40) von Ammon, R.; Fischer, R. D. *Angew. Chem., Int. Ed.* **1972**, *11*, 675–692.
(41) Sievers, R. E. *Nuclear Magnetic Resonance Shift Reagents*; Academic Press: New York, 1973.

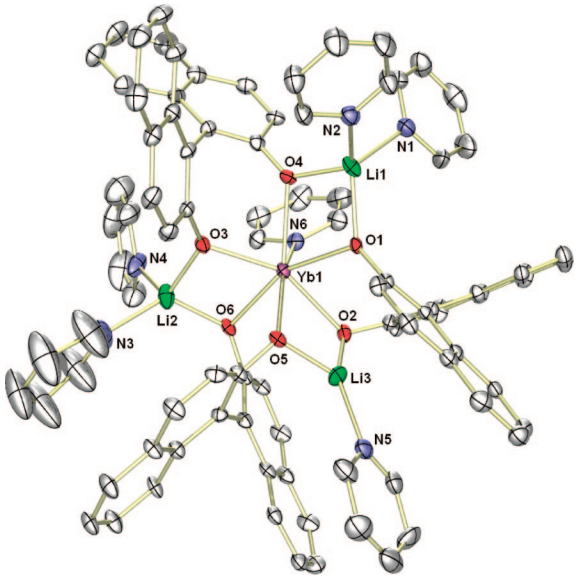

Figure 6. ORTEP of $Li_3(py)_5(BINOLate)_3Yb(py)$ (**4-Yb**) with 30% probability thermal ellipsoids.

tensor, where r is the distance from the lanthanide to the nucleus of interest in the bound substrate and θ is the angle between this vector and the principal molecular axis (Figure 9).[29,30,38,39,41–45] The magnitude of the LIS experienced by a substrate that binds reversibly to a paramagnetic lanthanide center is also dependent on the molar concentration ratio of the lanthanide shift reagent (SR) to the substrate and can often be obtained graphically as the slope of the observed chemical shift (δ_{obs}) vs [SR]/[sub].[38,39,41,46,47]

Aspinall and Salvadori, and co-workers have demonstrated that the paramagnetic shifts of $Na_3(THF)_6(BINOLate)_3Yb$ are entirely dipolar in origin and that unpaired electrons are not delocalized onto the protons of the BINOLate ligands.[29,30] This is most likely true for other paramagnetic $M_3(THF)_n(BINOLate)_3Ln$ complexes.

The BINOLate 3,3′-hydrogens (Figure 9) of **1-Eu**, **1-Yb**, **1-Pr**, and **5-Eu** experience large LISs due to their proximity to the paramagnetic centers and resonate at 25.06, 88.56, −11.36, and 40.56 ppm (Table 4). The 9,9′-hydrogens also exhibit large LISs. Similarly, the diamine resonances in **5-Eu** experience significant LISs to lower frequencies, as seen in the ^{1}H NMR spectrum in Figure 7. The diamine backbone hydrogens are diastereotopic due to the chirality of the complexes (see Figures 7 and 8). The diastereotopicity of the protons in the ethylene backbone in **5-Eu** could arise from tight binding of the diamine to the lithium centers. Rapid and reversible dissociation of the diamine, however, would *not* render the diamine backbone hydrogens equivalent, as observed in the free diamine, because the diamine nitrogens must each adopt the (*S*)-configuration when binding to the complex composed of (*R*)-BINOLate ligands. Diamine dissociation would, however, result in a smaller LIS. Evidence to support tight binding of the diamine is presented in the sections that follow.

2.4. Examination of Solution Binding of Substrates and Substrate Analogues to 1-Ln and 5-Ln Complexes. This section describes the first definitive evidence that the lanthanide in **1-Ln** can bind organic Lewis bases in solution. It will also be shown that the most important factor in predicting the lanthanide's affinity to bind Lewis bases in the series of $M_3(THF)_n(BINOLate)_3Ln$ complexes is not the lanthanide ionic radii but the size of the main group metal.

Prior investigations to probe substrate binding in $M_3(THF)_n(BINOLate)_3Ln$ complexes involved the use of paramagnetic Pr, Eu, and Yb derivatives. Previously reported ^{1}H NMR binding studies of $Na_3(THF)_6(BINOLate)_3Ln$ [Ln = Pr and Eu] with cyclohexenone exhibited small chemical shift differences for the α-vinyl proton, on the order of 0.1 ppm or less.[15] Similarly, addition of pivalaldehyde to **1-Pr** resulted in a shift of only 0.1 ppm for the formyl C−H proton.[16] These small shifts could be attributed to coordination of the carbonyls to the main group metals. Experimental error in the measured LIS in THF-d_8 arises from referencing of the NMR spectra to residual protons in the THF-d_8 solvent. Binding of THF solvent to the paramagnetic complexes results in a LIS of the residual protio solvent resonances (see the structures of **2-Eu** and **2-Pr**).[34]

A comparison of cyclohexenone binding to $Li_3(THF)_n(BINOLate)_3Eu$ (**1-Eu**) and $Li_3(DMEDA)_3(BINOLate)_3Eu$ (**5-Eu**) could reveal whether the carbonyl group binds to the lithium or the lanthanide centers. If cyclohexenone binds to the lithium centers, the LISs of **1-Eu** and **5-Eu** will be significantly different, because the lithium centers in DMEDA adduct **5-Eu** are coordinatively saturated and cannot bind cyclohexenone without dissociation of DMEDA. In contrast, if binding takes place at the lanthanide center, cyclohexenone will exhibit similar LISs with both **1-Eu** and **5-Eu**. Addition of 6 equiv of cyclohexenone to **1-Eu** in THF-d_8 resulted in LISs of the α- and β-vinyl hydrogens to *higher frequencies*, giving chemical shift differences of 0.56 and 0.16 ppm, respectively, consistent with reversible substrate binding (Table 5, entry 1). At a similar concentration ratio of **5-Eu**, the cyclohexenone α- and β-vinyl resonances also shifted to higher frequencies, giving LISs of 0.66 and 0.18 ppm (entry 2). These shifts can be easily seen in the vinyl section of the stacked ^{1}H NMR spectra of cyclohexenone, cyclohexenone + **1-Eu**, and cyclohexenone + **5-Eu** in Figure 10, where the α- and β-hydrogens have been highlighted. These results provide the first evidence for solution binding of Lewis bases to the lanthanide center in Shibasaki's catalysts. In all the binding studies herein, chemical shift values were referenced to a non-coordinating internal standard (mesitylene).

Further support for substrate binding was obtained using **1-Pr**, which induced LISs to *lower frequencies* for the α- and β-vinyl hydrogens of cyclohexenone of 0.46 and 0.28 ppm, respectively (Table 5, entry 3).[34] It is known that substrate binding to isostructural europium and praseodymium complexes exhibits LISs in opposite directions.[38,39] The magnitude of the LISs observed with cyclohexenone and **1-Eu**, **1-Pr**, and **5-Eu** *can only arise from binding of the carbonyl oxygen to the lanthanide centers*. To put the observed LISs in perspective, LISs of cyclohexenone were examined in the presence of the well-known chiral shift reagent $Eu(hfc)_3$ [hfc = heptafluoropropylhydroxymethylene-(+)-camphorate].[34,38,40] At a similar concentration ratio in THF-d_8, $Eu(hfc)_3$ caused only a small LIS in the α-vinyl hydrogen of cyclohexenone (0.05 ppm, entry 6). Increasing the concentration of $Eu(hfc)_3$ to bring this mixture to a 1:1 molar ratio resulted in a LIS of 0.30 ppm (entry 7). These shifts are smaller than would be observed

(42) Montaudo, G.; Librando, V.; Caccamese, S.; Maravigna, P. *J. Am. Chem. Soc.* **1983**, *95*, 6365–6370.
(43) Bertini, I.; Luchinat, C. *Coord. Chem. Rev.* **1996**, *150*, 29–75.
(44) Di Bari, L.; Salvadori, P. *Coord. Chem. Rev.* **2005**, *249*, 2854–2879.
(45) Montaudo, G.; Librando, V.; Caccamese, S.; Maravigna, P. *J. Am. Chem. Soc.* **1973**, *95*, 6365–6370.
(46) Midland, M. M.; Koops, R. W. *J. Org. Chem.* **1990**, *55*, 4647–4650.

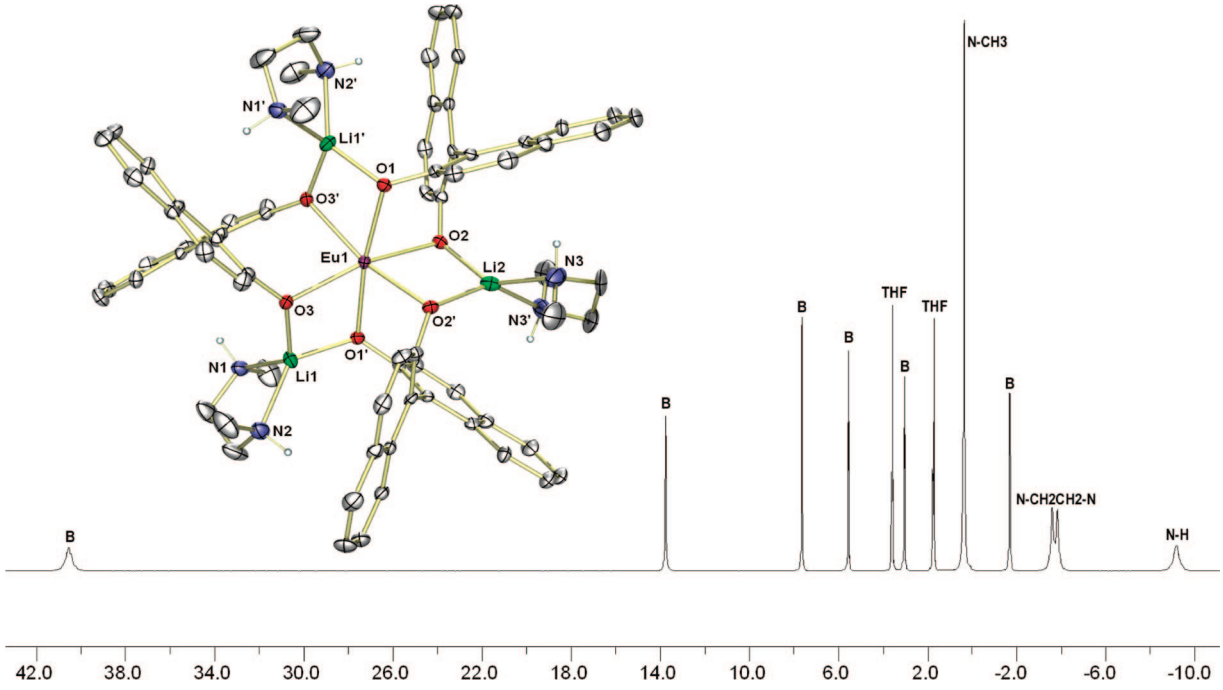

Figure 7. ^{1}H NMR spectrum of **5-Eu** in THF-d_8 and ORTEP with 30% probability thermal ellipsoids. (See Supporting Information for details of isostructural **5-Lu**, **5-La**, and **5-Y**.) B = Binolate ligand resonance.

Table 3. Selected Bond Distances (Å) for $Li_3(DMEDA)_3(BINOLate)_3Ln$ Complexes **5-Lu**, **5-Eu**, **5-La**, and **5-Y**

compound	Ln−O (Å)	Li−N (Å)
$Li_3(DMEDA)_3(BINOLate)_3Lu$ (**5-Lu**)	Lu1−O3, 2.189(4)	Li1−N1, 2.034(11)
	Lu1−O3, 2.189(4)	Li1−N2, 2.138(11)
	Lu1−O1, 2.192(3)	Li2−N3, 2.134(14)
	Lu1−O1, 2.192(3)	Li2′−N3′, 2.107(14)
	Lu1−O2, 2.210(3)	Li1′−N1′, 2.100(10)
	Lu1−O2, 2.210(3)	Li1′−N2′, 2.106(9)
$Li_3(DMEDA)_3(BINOLate)_3Eu$ (**5-Eu**)	Eu1−O2, 2.290(3)	Li1−N1, 2.101(9)
	Eu1−O2, 2.290(3)	Li1−N2, 2.072(9)
	Eu1−O3, 2.302(4)	Li2−N3, 2.062(14)
	Eu1−O3, 2.302(4)	Li2′−N3′, 2.117(12)
	Eu1−O1, 2.306(3)	Li1′−N1′, 2.114(9)
	Eu1−O1, 2.306(3)	Li1′−N2′, 2.133(8)
$Li_3(DMEDA)_3(BINOLate)_3La$ (**5-La**)	La1−O2, 2.399(4)	Li1−N1, 2.094(10)
	La1−O2, 2.399(4)	Li1−N2, 2.063(10)
	La1−O3, 2.402(4)	Li2−N3, 2.059(13)
	La1−O3, 2.402(4)	Li1′−N3′, 2.106(12)
	La1−O1, 2.412(3)	Li2′−N1′, 2.109(10)
	La1−O1, 2.412(3)	Li2′−N2′, 2.130(10)
$Li_3(DMEDA)_3(BINOLate)_3Y$ (**5-Y**)	Y1−O1, 2.2311(19)	Li1−N1, 2.056(6)
	Y1−O1, 2.2311(19)	Li1−N2, 2.119(7)
	Y1−O3, 2.241(2)	Li2−N3, 2.120(7)
	Y1−O3, 2.241(2)	Li2′−N3′, 2.099(7)
	Y1−O2, 2.2529(18)	Li1′−N1′, 2.112(6)
	Y1−O2, 2.2529(18)	Li1′−N2′, 2.112(6)

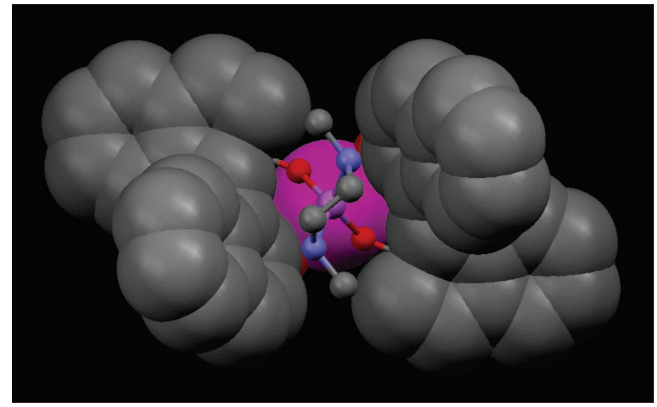

Figure 8. View of a partial structure of the diamine bound to lithium (small purple sphere) between BINOLate ligands in **5-La**. The lanthanide (large sphere) is lavender, the oxygens are red, and the nitrogens are violet.

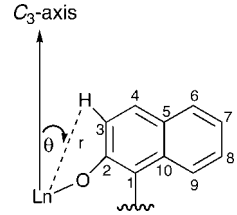

Figure 9. Diagram illustrating the numbering system and the geometrical parameters used in the analysis of ^{1}H NMR spectra of paramagnetic Ln complexes.

in non-coordinating solvents due to competition between THF-d_8 and cyclohexenone for binding at the europium center. We attribute the larger LISs of **1-Eu** and **5-Eu** over $Eu(hfc)_3$ to the greater steric congestion about the lanthanide centers of **1-Eu** and **5-Eu**, resulting in a higher selectivity for the smaller carbonyl oxygen over the THF oxygen.[41] For comparison, diamagnetic **5-La** and $(BINOLate)Li_2$ induced shifts of <0.03 ppm in the vinyl cyclohexenone resonances (entries 8 and 9). This comparison highlights the utility of paramagnetic complexes in NMR binding studies.

(47) Montaudo, G.; Finocchiaro, P. *J. Org. Chem.* **1972**, *37*, 3434–3439.

Table 4. ^{1}H NMR Data for Select Compounds[a]

compound	^{1}H (ppm) BINOLate	N−H	N−CH_2CH_2−N	Me
DMEDA	−	1.18 s	2.56 s	2.33 s
(BINOLate)Li_2	7.62–6.62 br-m	−	−	−
$Li_3(THF)_4(BINOLate)_3Eu$ (**1-Eu**)	25.06 br s (H **3**); 10.81 br s (H **4**); 7.48 d (H **6**); 6.18 t (H **7**); 3.94 t (H **8**); 0.545 d (H **9**)	−	−	−
$Li_3(THF)_4(BINOLate)_3Yb$ (**1-Yb**)	88.56 br s (H **3**); 23.74 br s (H **4**); 8.31 d (H **6**); 2.95 br s (H **7**); −1.02 br s (H **8**); −13.45 br s (H **9**)	−	−	−
$Li_3(THF)_4(BINOLate)_3Pr$(**1-Pr**)	14.34 br-d (H **9**); 9.96 br-t (H **8**); 8.34 br-t (H **7**); 7.76 br-d (H **6**); 3.68 br s (H **4**); −11.36 br s (H **3**)	−	−	−
$Li_3(DMEDA)_3(BINOLate)_3Eu$ (**5-Eu**)	40.56 br s (H **3**); 13.76 br s (H **4**); 7.65 d (H **6**); 5.56 t (H **7**); 3.04 t (H **8**); −1.69 d (H **9**)	−9.16 br s	−3.82 br s; −3.59 br s	0.37 s
$Li_3(DMEDA)_3(BINOLate)_3La$ (**5-La**)	6.83 d, 2 H; 6.91 m, 4 H; 7.23 d, 2H; 7.67 t, 4 H	0.61 br s	1.69 br-d; 1.96 br-d	1.60 s

[a] For Numbering of the BINOLate Ligand, see Figure 9. Assignments are Based on Literature Values and Two-dimensional Spectroscopy [COSY, HMQC, HMBC and NOESY].[11,15,29,30] Solvent: THF-d_8 at $\delta = 3.58$ and 1.73. Assignments based on a comparison with literature values.[11,15,29,30]

Table 5. Comparison of Measured LISs of Cyclohexenone and DMF with Various Shift Reagents and Shifts on Coordination with Some Diamagnetic Species[a]

entry	shift reagent and substrate	[SR]/[Sub] (molar ratio)	[Sub]:[SR]	LIS $\Delta\delta$ H_α (ppm)	$\Delta\delta$ H_β (ppm)	$\Delta\delta$ H (formyl) (ppm)	$\Delta\delta CH_3$ (ppm)	$\Delta\delta$ CH_3 (ppm)
1	**1-Eu** + cyclohexenone	0.032 M/0.193 M	6.0	0.56	0.16	−	−	−
2	**5-Eu** + cyclohexenone	0.037 M/0.186 M	5.0	0.66	0.18	−	−	−
3	**1-Pr** + cyclohexenone	0.032 M/0.193 M	6.0	0.46	0.28	−	−	−
4	**1-Yb** + cyclohexenone	0.032 M/0.193 M	6.0	0.26	0.06	−	−	−
5	**1-Yb** + cyclohexenone	0.064 M/0.193 M	3.0	0.57	0.14	−	−	−
6	$Eu(hfc)_3$ + cyclohexenone	0.032 M/0.193 M	6.0	0.05	0.00	−	−	−
7	$Eu(hfc)_3$ + cyclohexenone	0.193 M/0.193 M	1.0	0.30	0.06	−	−	−
8	**1-La** + cyclohexenone	0.032 M/0.194 M	6.1	0.03	0.02	−	−	−
9	(BINOLate)Li_2 + cyclohexenone	0.032 M/0.193 M	6.0	0.03	0.02	−	−	−
10	**1-Eu** + DMF	0.032 M/0.258 M	8.1	−	−	1.14	1.26	0.61
11	**5-Eu** + DMF	0.032 M/0.258 M	8.1	−	−	2.30	1.06	0.77
12	**1-Yb** + DMF	0.032 M/0.258 M	8.1	−	−	4.27	2.43	1.45
13	**1-La** + DMF	0.032 M/0.258 M	8.1	−	−	0.09	0.04	0.02
14	(BINOLate)Li_2 + DMF	0.032 M/0.258 M	8.1	−	−	0.09	0.04	0.03

[a] Internal reference: mesitylene at $\delta = 6.73$ (C−H) and $\delta = 2.22$ (CH_3). Solvent: THF-d_8 at $\delta = 3.58$ and 1.73.

Aldehydes are also important substrates for reactions catalyzed by **1-Ln** complexes.[1,6,27,48,49] A good model for aldehyde substrates is DMF, which binds more tightly to lanthanides than aldehydes due to the increased basicity of the amide carbonyl oxygen. Addition of 8 equiv of DMF to both **1-Eu** and **5-Eu** resulted in LISs of the formyl hydrogen of 1.14 and 2.30 ppm, respectively (Table 5, entries 10 and 11).[34] We attribute the greater LISs of DMF with **5-Eu** relative to **1-Eu** to a greater selectivity for the smaller binding pocket of the DMEDA adduct. Note that all four of the DMEDA complexes crystallized from THF as 6-coordinate lanthanide complexes, whereas **1-La**, **1-Pr**, and **1-Eu** crystallized with lanthanide-bound THF solvents.[41,34] Addition of DMF to diamagnetic (BINOLate)Li_2 and **1-La** resulted in shifts of <0.09 ppm (entries 13 and 14, respectively).

Based on reports that the small Yb center in $M_3(THF)_6$-(BINOLate)$_3$Yb [M = Na and K] does not even bind water,[30,33] we examined binding of cyclohexenone to the paramagnetic-lithium analogue $Li_3(THF)_6(BINOLate)_3Yb$ (**1-Yb**). When cyclohexenone (6 equiv) was combined with **1-Yb**, a LIS of 0.26 ppm was obtained for the α-vinyl resonance (Table 5, entry 4). Doubling the concentration of **1-Yb** produced a LIS of 0.57 ppm for the α-vinyl proton (entry 5). Utilizing 8 equiv of DMF and **1-Yb** resulted in a LIS of the formyl hydrogen of 4.27 ppm (entry 12). Our solution studies with **1-Yb** stand in contrast to those with the heavier main group analogues, $M_3(THF)_n$-(BINOLate)$_3$Yb (M = Na and K).[30,33] Our results indicate that the *overriding factor in controlling the binding ability of $M_3(THF)_n(BINOLate)_3Ln$ complexes is the radius of the main group metal and not the lanthanide ionic radius*, as previously proposed.[30] Further support for this hypothesis was gained in binding studies with a series of $M_3(THF)_6(BINOLate)_3Ln$ complexes (M = Na and K), which do not bind organic ligands at the lanthanide.[35]

To probe the solution binding of softer ligands to the lanthanide centers, we also examined the interaction of pyridine with **1-Eu**, **1-Yb**, and **5-Eu** (Table 6). Addition of pyridine (6 equiv) to solutions of these complexes resulted in significant LISs of the aromatic pyridine protons. In particular, at a concentration ratio of 0.064 M/0.193 M, the **1-Yb** complex produced a LIS of 0.39 ppm for the 2,6-hydrogens of pyridine. The observed LISs are consistent with binding of pyridine to the Eu and Yb centers and are in line with the results of the cyclohexenone and DMF binding studies above.

2.5. Competitive Binding Studies. In the competitive binding studies of this section, the interaction of **5-Eu** with cyclohexenone is examined in greater depth to gain insight into the origin of the observed LISs. Additionally, experiments are outlined to probe the binding of DMEDA to lithium in **5-Eu**.

The interpretation of LISs can be complicated by several factors, including line broadening caused by fast exchange of bound and free substrate, the presence of impurities, different structures, or conformational changes, which can result in signal

(48) Shibasaki, M.; Sasai, H.; Arai, T.; Iida, T. *Pure Appl. Chem.* **1998**, *70*, 1027–1034.
(49) Shibasaki, M.; Kanai, M.; Matsunaga, S. *Aldrichim. Acta* **2006**, *39*, 31–39.

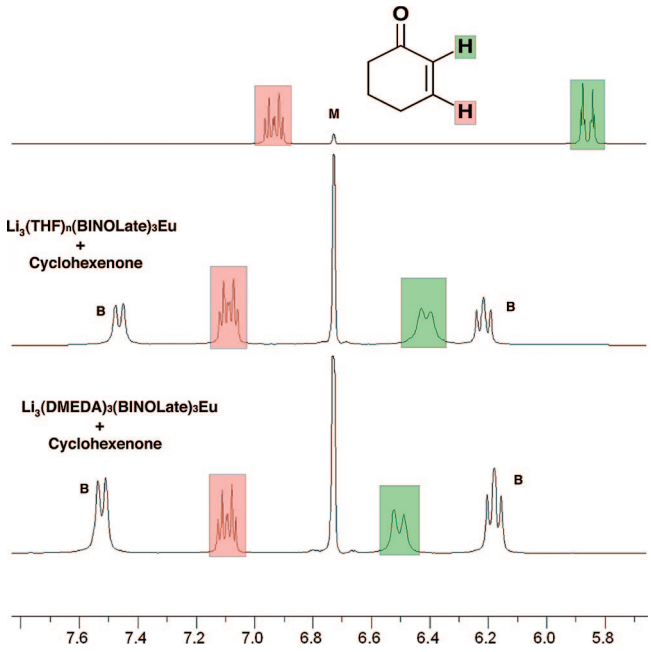

Figure 10. Stack plot of the ^{1}H NMR spectra of the vinyl region of cyclohexenone (top) and cyclohexenone in the presence of $Li_3(THF)_n$-$(BINOLate)_3Eu$ (middle) and $Li_3(DMEDA)_6(BINOLate)_3Eu$ (bottom). The α- and β-hydrogens are highlighted in green and pink, respectively. Resonances of BINOLate hydrogens are labeled B, and the mesitylene internal standard is labeled M.

Table 6. Measured LISs of Pyridine with **1-Eu**, **1-Yb**, and **5-Eu** at Similar Concentration Ratios[a]

			LIS			
				Δδ H (ppm)		
entry	shift reagent and substrate (pyridine)	[SR]/[Sub] (molar ratio)	[Sub]:[SR]	*ortho*	*meta*	*para*
1	**1-Eu** + pyridine	0.032 M/0.193 M	6.0	1.90	0.63	0.63
2	**5-Eu** + pyridine	0.031 M/0.187 M	6.0	1.03	0.02	0.38
3	**1-Yb** + pyridine	0.032 M/0.193 M	6.0	0.20	0.04	0.06
4	**1-Yb** + pyridine	0.064 M/0.193 M	3.0	0.39	0.07	0.13

[a] Internal reference: mesitylene at $\delta = 6.73$ (H) and $\delta = 2.22$ (CH_3). Solvent: THF-d_8 at $\delta = 3.58$ and 1.73.

averaging and line broadening.[38,40,41,45,47] Complications can also arise when shift reagents have multiple binding sites.[39,41] Any significant contributions of other structures or impurities to the observed LIS should result in the deviation of plots of δobs vs [SR]/[cyclohexenone] from linearity.[39,41,46,47]

To determine if the observed LISs with cyclohexenone are primarily due to the formation of a single species, binding studies were performed by maintaining the concentration of cyclohexenone and increasing the concentration of $Li_3(DMEDA)_3(BINOLate)_3Eu$ (**5-Eu**). Plots of δobs vs [SR]/[cyclohexenone] for the α- and β-vinyl protons are linear, with slopes for H_α and H_β of 0.47 and 0.16 ppm, respectively (Figure 11), suggesting that binding occurs only at the lanthanide center in **5-Eu**. Furthermore, the linearity of these plots, with correlation coefficients >0.98, indicates that the shifts do not arise from an averaging over many significantly different structures and that the diamines are bound under these conditions.[38,41,46,47]

Although the structures and binding experiments presented above indicate that the diamine coordinates to the lithium centers, it is conceivable that the diamine could be partially displaced by the substrate analogues. As mentioned, reversible binding of the diamine to enantioenriched **5-Eu** would *not* result in coalescence

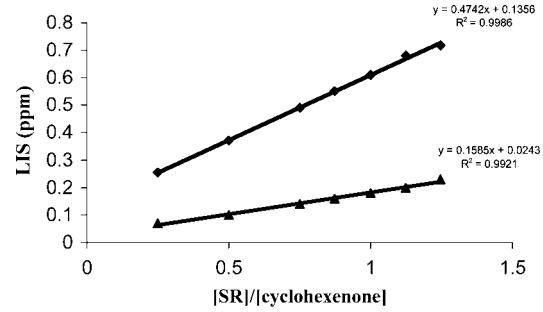

Figure 11. Measured induced shifts of H_α (◆) and H_β (▲) of cyclohexenone as a function of the concentration of **5-Eu** at 0.0065, 0.0130, 0.0195, 0.0227, 0.0260, 0.0292, and 0.0324 M with a fixed cyclohexenone concentration of 0.026 M. The spectra were acquired in THF-d_8 referenced to mesitylene.

of the diamine methylene resonances, because the diamine must bind with the (*S*,*S*)-configuration at nitrogen to the (*R*)-BINOLate-based complex (Figure 8). Displacement of the diamine, however, would result in reduced LISs. As outlined in Figure 9, geometrical changes at the lanthanide center also cause changes in the magnitude of the LIS. It is noteworthy that the diamine in **5-Eu** exhibits large LISs in THF-d_8, which can only occur if the affinity of the lithium for the diamine is high.

We next examined the interaction of free diamine with **5-Eu**. The proton resonances for unbound DMEDA in THF-d_8 appear at 1.18 (s, N−H), 2.33 (s, Me), and 2.56 ppm (s, CH_2CH_2). The diamine resonances of **5-Eu** experience relatively large LISs to lower frequencies and appear at −9.16 (s, N−H) and 0.37 ppm (s, Me), and the diastereotopic methylene resonances are broad singlets at −3.82 and −3.59 ppm. To examine the possibility of exchange of bound and free DMEDA, 6 equiv of DMEDA was combined with **5-Eu** in THF-d_8 at a concentration ratio of 0.031 M/0.187 M. Under these conditions, only one set of diamine resonances was observed [−2.76 (s, N−H), 1.59 (s, Me), and 0.22 ppm (br s, CH_2CH_2)]. The coalescence of free and bound diamine is consistent with rapid diamine exchange on the ^{1}H NMR time scale.

To examine the possibility of dissociation of the diamine ligand and coordination of DMF to lithium, we examined the binding of DMF to **5-Eu** in THF-d_8 first in the absence of additional DMEDA and second in the presence of 5 equiv of DMEDA. If DMF is competitive with DMEDA for the lithium centers in **5-Eu**, the LIS of DMF should change when the concentration of DMEDA is increased, because the equilibrium between lithium-bound DMF and DMEDA would be shifted toward the DMEDA adduct. The DMF resonances should then exhibit a change in the LIS. In contrast, if there were no change in the DMF resonances with the increased DMEDA concentration, the conclusion would be that DMF does not compete with DMEDA for the lithium centers. With this in mind, 4 equiv of DMF was combined with **5-Eu** in THF-d_8 (DMF/Eu = 0.129 M/0.032 M), resulting in a LIS of 5.42 ppm for the formyl hydrogen. Due to a geometrical change on going from 6- to 7-coordinate,[50] the diamine resonances shifted to −3.86 (s, N−H), 0.92 (s, Me), −0.25, and −0.51 ppm (two br s, CH_2CH_2).

Next, 5 equiv of DMEDA was added to the sample, resulting in coalescence of free and bound diamine peaks, with resonances shifted to −1.07 (s, N−H), 1.68 (s, Me), 1.30, and 1.21 ppm (two br s, CH_2CH_2). In contrast, no significant change in the

(50) Kowall, T.; Foglia, F.; Helm, L.; Merbach, A. E. *J. Am. Chem. Soc.* **1995**, *117*, 3790–3799.

LIS of the DMF formyl hydrogen was observed (5.48 ppm, 1% change) upon addition of the 5 equiv of diamine. Two important conclusions can be drawn from these binding studies. First, DMF displays high selectivity for the lanthanide center and has little or no interaction with the lithium centers in **5-Eu**. Second, the diamine does not bind to the lanthanide center to any appreciable extent, because no change in the LIS of the DMF formyl hydrogen was observed upon addition of 5 equiv of DMEDA to **5-Eu**. Thus, the DMEDA and DMF exhibit orthogonal binding to these heterobimetallic complexes.

2.6. Examination of $Li_3(DMEDA)_3(BINOLate)_3La$ (5-La) in Catalytic Asymmetric Reactions. The binding studies above clearly demonstrate that the DMEDA adduct **5-Eu** binds Lewis basic substrates and substrate analogues at the lanthanide center. An important question remains: Do the DMEDA adducts catalyze asymmetric reactions? To explore this question, we focused on the lanthanum derivative $Li_3(THF)_n(BINOLate)_3Ln$ (**1-La**) because it often exhibits the highest enantioselectivities.[6]

We examined $Li_3(DMEDA)_3(BINOLate)_3La$ (**5-La**) in three catalytic asymmetric reactions that are mechanistically distinct and compared our results to those reported by Shibasaki and co-workers with $Li_3(THF)_n(BINOLate)_3La$ (**1-La**). The phosphonylation of aldehydes, the asymmetric Henry reaction, and the Diels–Alder reaction are catalyzed by **1-La**. Reaction of 1.2 equiv of dimethyl phosphite with benzaldehyde[20] was performed in the presence of 10 mol % **5-La** at −78 °C in THF (eq 3). After workup, the α-hydroxy phosphonate product was isolated in 92% yield with 78% ee, almost the same enantioselectivity as reported for **1-La** by Shibasaki (eq 3). In the asymmetric Henry reaction (eq 4),[51] 10 equiv of nitromethane was added to benzaldehyde in the presence of 10 mol % **5-La** at −50 °C in THF. Under these conditions, the nitroaldol product was isolated in 76% yield with 25% ee. Shibasaki reported that **1-La** gave product of 38% ee. Finally, addition of 10 equiv of cyclopentadiene to the dieneophile 3-(1-oxo-2-propenyl)-2-oxazolidinone in CH_2Cl_2 at 0 °C in the presence of 10 mol % DMEDA adduct **5-La** produced the Diels–Alder product in 54% yield with 32% ee (eq 5), which is essentially the same enantioselectivity reported by Shibasaki and co-workers with **1-La**.[28] Although we have not yet studied the reaction mechanisms in eqs 3–5, it seems unlikely that the DMEDA ligands completely dissociated from **5-La** to generate **1-La**, which then catalyzed the reactions. One explanation for the similarities in enantioselectivities with **5-La** and **1-La** in eqs 3–5 is that the DMEDA ligands are sandwiched between the BINOLate ligands and do not project toward the lanthanide binding site, as seen in Figure 8.

2.7. Reaction of Ethylene Diamine with 1-Eu. The preferential coordination of DMEDA to the lithium centers in **5-Eu** contrasts with the binding of pyridine to both the lanthanide and lithium centers in **3-La**, **4-Eu**, and **4-Yb**. This difference was attributed to the greater steric hindrance of the DMEDA nitrogens relative to pyridine.[52] To probe binding of the smaller bidentate diamine in this system, **1-Eu** was combined with 4 equiv of ethylene diamine (en). The proton resonances for free en [1.19 (N−H) and 2.56 ppm (−CH_2CH_2−)] in THF-d_8 exhibited significant *downfield* LISs to 5.61 (br s, N−H) and 3.92 ppm (br s, −CH_2CH_2−) in the presence of **1-Eu**. Contrary to our observations with **5-Eu**, which resulted in LISs of the DMEDA resonances to lower frequency, the en resonances were shifted to *higher frequency*, as were the resonances for the substrate analogues (see Table 5 for cyclohexenone and DMF and Table 6 for pyridine). The direction and magnitude of the LISs suggest

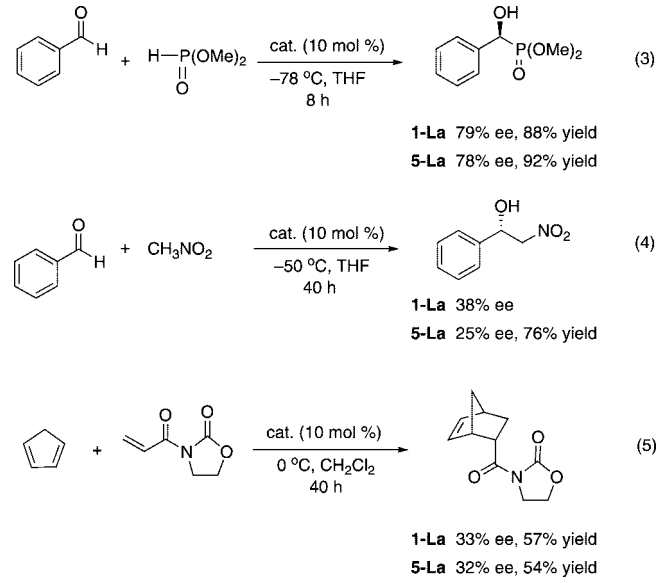

that en is interacting directly with the paramagnetic europium center as well as the lithium centers.

To probe the interaction of en with heterobimetallic **1-Eu**, en and **1-Eu** were combined (Eu:en = 1:4) in THF, and pentane was diffused into the solution at room temperature by vapor diffusion. The resulting pale yellow crystals of **6-Eu** were analyzed by X-ray diffraction at low temperature. As hinted by the ^{1}H NMR LISs of en, the structure consists of both Eu and Li bound diamines and is dimeric, with a bridging en ligand bonded to both europium centers (Figure 12). The Eu−N distances in **6-Eu** [2.601(6) and 2.582(4) Å] are slightly longer than in the 7-coordinate pyridine adduct **4-Eu** [2.578(5) Å]. In the dimer, the lithium centers exhibit three different bonding modes to the en ligands. Three lithiums contain chelating en ligands, as observed in the DMEDA ligands in **5-Eu**. One lithium binds two en ligands in a monodentate fashion, and the other two lithiums have disordered en ligands with partial occupancy for the monodentate and chelating binding modes. The Li−N distances in **6-Eu** are similar to the Li−N distances in **5-Eu** [2.062(14)−2.101(9) Å].

The observation that en does not chelate to the Eu centers in $[Li_6(en)_7(BINOLate)_6Eu_2][\mu\text{-}\eta^1,\eta^1\text{-en}]$ (**6-Eu**), coupled with the binding of the two pyridine ligands in **3-La** in a pseudo-*trans* fashion, lead us to propose that **1-Ln** complexes *do not readily bind bidentate substrates in a chelating fashion at the lanthanide center*. Although the en ligand readily chelates, binding to the lanthanide in a chelating fashion or binding of two monodentate ligands in a *cis* fashion would create greater repulsive interactions between the BINOLate ligands by forcing them together into a smaller volume.

3. Conclusions

At the outset of the investigations reported herein, direct experimental evidence that the lanthanide in Shibasaki's $Li_3(THF)_n(BINOLate)_3Ln$ (**1-Ln**) catalysts could bind Lewis basic substrates and their analogues was lacking. By careful crystallization of heterobimetallic compounds **1-Ln** from Lewis

(51) Arai, T.; Yamada, Y. M. A.; Yamamoto, N.; Sasai, H.; Shibasaki, M. *Chem. Eur. J.* **1996**, *2*, 1368–1372.
(52) Seligson, A. L.; Trogler, W. C. *J. Am. Chem. Soc.* **1991**, *113*, 2520–2527.

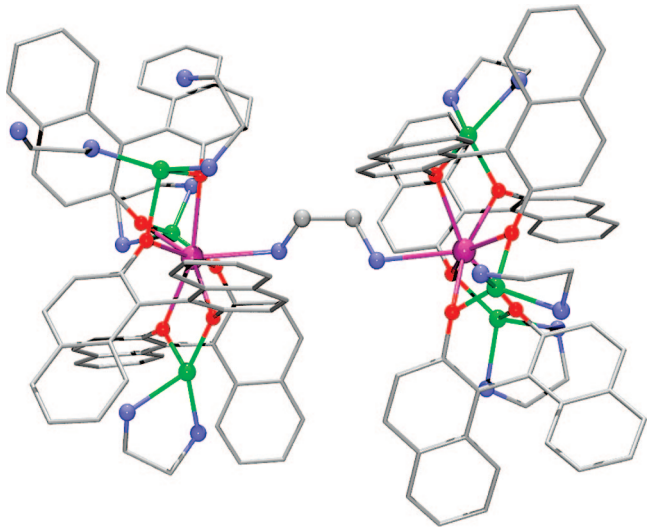

Figure 12. Structure of $[Li_6(en)_7(BINOLate)_6Eu_2][\mu\text{-}\eta^1,\eta^1\text{-en}]$ (**6-Eu**). Selected bond distances [Å]: Eu1−N1, 2.601(6); Eu2−N2, 2.582(4); Eu1−O1, 2.377(4); Eu1−O2, 2.302(4); Eu1−O3, 2.377(4); Eu1−O4, 2.336(4); Eu1−O5, 2.392(4); Eu1−O6, 2.315(4); Eu2−O7, 2.309(4); Eu2−O8, 2.419(4); Eu2−O9, 2.340(4); Eu2−O10, 2.378(4); Eu2−O11, 2.307(4); Eu2−O12, 2.376(4); Li1−N3, 2.092(12); Li1−N4, 2.129(13); Li2−N5, 2.13(2); Li2−N7, 2.16(2); Li3−N9, 2.12(2); Li3−N10, 1.92(2); Li4−N14, 1.96(2); Li4−N15, 2.12(2); Li5−N18, 1.98(2); Li5−N19, 2.122(14); Li6−N22, 2.090(13); Li6−N23, 2.110(14).

basic solvents (THF or pyridine), 7-coordinate $Li_3(THF)_4(BINOLate)_3Ln(THF)$ (**2-Eu**, **2-Pr**, **2-La**) and $Li_3(py)_5(BINOLate)_3Ln(py)$ (**4-Eu** and **4-Yb**) and 8-coordinate $Li_3(py)_5(BINOLate)_3La(py)_2$ (**3-La**) were isolated and crystallographically characterized. These structures demonstrate that the lanthanides in **1-Ln** can bind Lewis bases in the solid state. The isolation of the THF adducts **2-Ln** (Ln = Eu, Pr, and La) also indicates that THF, the solvent of choice for Shibasaki's catalytic reactions, is a competitive binder.

To perform solution studies, it was necessary to differentiate between binding at the Lewis acidic lithiums and binding at the lanthanide. This was accomplished by synthesis of the DMEDA derivatives $Li_3(DMEDA)_3(BINOLate)_3Ln$ (**5-Ln**). Comparison of LISs with three Lewis bases in the presence of **1-Eu** and **5-Eu** provided the first definitive evidence that the lanthanide in **1-Ln** can bind and, therefore activate, organic Lewis bases. Previously, it was believed that the most important factor in determining binding ability of $M_3(THF)_6(BINOLate)_3Ln$ complexes was the radius of the lanthanide.[30] This hypothesis was based on the observation that $M_3(THF)_6(BINOLate)_3Yb$ (M = Na and K) complexes do not bind Lewis bases in solution or the solid state, in contrast to larger lanthanide analogues, which do bind water. We found, however, that the lithium analogue **1-Yb** binds pyridine in the solid state and cyclohexenone, DMF, and pyridine in solution. Thus, while lanthanide radius is an important factor, the *radius of the main group metal plays a larger role in determining binding ability than the size of the lanthanide*.[35]

Our observation that $Li_3(py)_5(BINOLate)_3La(py)_2$ (**3-La**) binds two pyridine ligands in a pseudo-*trans* fashion, coupled with the binding of en through a single nitrogen to each europium center (rather than chelating) in the dimer $[Li_6(en)_7(BINOLate)_6Eu_2][\mu\text{-}\eta^1,\eta^1\text{-en}]$, supports our hypothesis that the lanthanide in Shibasaki's $Li_3(THF)_n(BINOLate)_3Ln$ catalysts is reluctant to chelate bidentate substrates. Finally, it is conceivable that the catalyst formed from $Li_3(THF)_n(BINOLate)_3La$ and water or other Lewis basic additives often affords the highest enantioselectivities,[6,53,54] because the large radius of the lanthanum catalyst can more readily achieve a coordination number of 8. In 8-coordinate $Li_3(sol)_n(BINOLate)_3La(S)L$ (L = additive, S = substrate), the substrate is held closer to the BINOLate ligands, because the lanthanide exhibits little or no displacement from the Li_3 plane. On the other hand, in the 7-coordinate adducts, the lanthanide and bound substrate are displaced from the Li_3 plane by as much as 0.76 Å (**2-La**).[35]

Shibasaki's heterobimetallic complexes comprise one of the most successful classes of asymmetric catalysts known. The results of this study expand our understanding of these important catalysts and will facilitate reaction optimization with these heterobimetallics and development of related multifunctional catalysts.

4. Experimental Section

4.1. General Methods. All reactions and manipulations were carried out under an inert atmosphere in a Vacuum Atmospheres drybox with attached MO-40 Dritrain, or by using standard Schlenk or vacuum line techniques with oven-dried glassware. Dichloromethane, toluene, and hexanes (UV grade, alkene-free) were dried through alumina columns under nitrogen. Diethyl ether and tetrahydrofuran were predried through alumina columns and further dried using sodium/benzophenone ketyl. Pentane (HPLC grade) was dried using sodium/benzophenone ketyl. Solutions were degassed as follows: they were cooled to −196 °C, evacuated under high vacuum, and thawed. This sequence was repeated three times in each case. Unless otherwise specified, all reagents were purchased from Aldrich Chemical Co., Acros, or Strem Chemicals, and all solvents were purchased from Fischer Scientific. High-purity and anhydrous $Ln(OTf)_3$ reagents were all purchased from Aldrich or Strem and used without purification. Deuterated solvents were purchased from Cambridge Isotopes. THF-d_8 was vacuum-transferred from sodium/benzophenone ketyl. *N*,*N*′-Dimethylethylene diamine (DMEDA) was dried over KOH, heated on an oil bath, and collected via fractional distillation under nitrogen. ^1H and $^{13}C\{^1H\}$ NMR spectra were obtained on a Bruker DMX-300 or on a Bruker AM-500 Fourier transform NMR spectrometer at 300 and 75 MHz or 500 and 125 MHz, respectively. Chemical shifts are recorded in units of parts per million downfield from tetramethylsilane and are reported relative to mesitylene internal standard in THF-d_8. All coupling constants are reported in hertz. The infrared spectra were obtained using a Perkin-Elmer 1600 series spectrometer. The asymmetric reactions in eqs 13 were performed following the procedures of Shibasaki and co-workers using **Eu-5**.[20,28,51]

4.2. General Procedure A: Synthesis of $Li_3(THF)_3(BINOLate)_3Ln$ (1-Ln) Complexes. 4.2.1. Synthesis of $Li_3(THF)_3(BINOLate)_3Pr$ (1-Pr). Li_2(*R*-BINOLate) (0.761 g, 2.55 mmol) was dissolved in 60 mL of THF, and $Pr(O_3SCF_3)_3$ (0.50 g, 0.850 mmol) was added as a solid in incremental portions to this clear solution. The reaction was allowed to stir for 3 days at room temperature inside the glovebox. The solution was then filtered through dry Celite, and all volatile materials were removed in vacuo. Dichloromethane (60 mL) was added to the remaining solid, the undissolved materials were removed by filtration through Celite, and the filtrate was recovered. The volatile materials were then removed from the filtrate, and the resulting solid was placed on a frit and washed with 2 mL of cold dry diethyl ether and three times with 5 mL of dry hexanes. Compound **1-Pr** (0.720 g) was obtained

(53) Yoshikawa, N.; Yamada, Y. M. A.; Das, J.; Sasai, H.; Shibasaki, M. *J. Am. Chem. Soc.* **1999**, *121*, 4168–4178.
(54) Yoshikawa, N.; Suzuki, T.; Shibasaki, M. *J. Org. Chem.* **2002**, *67*, 2556–2565.

as a white powder after drying under reduced pressure [69% yield based on $Pr(O_3SCF_3)_3$]. Pale X-ray-quality crystals were obtained via vapor diffusion of dry pentane into a THF solution of **1-Pr**: ^{1}H NMR (300 MHz, THF-d_8) $\delta = -11.36$ (br s, 2H), 3.68 (br s, 2H), 7.76 (br-d, $J = 6.5$ Hz, 2H), 8.34 (br-t, $J = 7.1$ Hz, 2H,), 9.96 (br s, 2H), 14.34 (br-d, $J = 5.1$ Hz, 2H); ^{13}C{^{1}H} NMR (75 MHz, THF-d_8) $\delta = 124.1$, 124.4, 126.3, 128.2, 129.3, 133.4, 135.4, 144.0, 147.6, and 176.6 ppm.

4.2.2. Synthesis of $Li_3(THF)_3(BINOLate)_3Yb$ (1-Yb). The synthesis of **1-Yb** was accomplished using general procedure A. The reagents were Li_2(*R*-BINOLate) (0.721 g, 2.42 mmol), $Yb(O_3SCF_3)_3$ (0.50 g, 0.806 mmol), and THF (60 mL). Compound **1-Yb** (0.749 g) was isolated in 73% yield based on $Yb(O_3SCF_3)_3$: ^{1}H NMR (300 MHz, THF-d_8) $\delta = -13.44$ (br s, 2H), -1.02 (br s, 2H), 2.95 (br s, 2H), 8.31 (d, $J = 8.1$ Hz, 2H,), 23.74 (br s, 2H), 88.59 (br s, 2H); ^{13}C{^{1}H} NMR (75 MHz, THF-d_8) $\delta = 56.6$, 108.0, 110.4, 114.1, 116.5, 122.1, 124.0, 124.7, 140.6, and 178.3 ppm; IR (KBr) $\nu = 3048$, 2956, 2873, 1615, 1591, 1558, 1502, 1464, 1425, 1341, 1278, 1249, 1143, 1071, 995, 957, 936, 860, 823, 746, 669, 576, 482 cm^{-1}. Anal. Calcd for $C_{72}H_{60}O_9Li_3Yb$: C, 68.46; H, 4.79. Found: C, 68.31; H, 4.88.[36]

4.3. General Procedure B: Crystallization of $Li_3(THF)_4(BINOLate)_3Ln(THF)$ (2-Ln) Complexes. Under a nitrogen atmosphere, 30 mg of $Li_3(THF)_3(BINOLate)_3Eu$ (**1-Eu**), $Li_3(THF)_3(BINOLate)_3Pr$ (**1-Pr**), or $Li_3(THF)_3(BINOLate)_3La$ (**1-La**) was added to a 4 mL vial and dissolved in 1.0 mL of anhydrous THF. The vial was then placed inside of a 20 mL screw-capped vial that was half-filled with dry pentane. After several days of pentane diffusion at room temperature, pale X-ray-quality crystals of compounds **2-Eu**, **2-Pr**, or **2-La** were obtained. These crystals were subjected to X-ray diffraction studies. NMR spectra of **2-Eu**, **2-Pr**, and **2-La** in THF-d_8 were identical to those of compounds **1-Eu**, **1-Pr**, and **1-La**, respectively.[11,15]

4.3.1. Crystallization of $Li_3(py)_5(BINOLate)_3La(py)_2$ (3-La). $Li_3(THF)_3(BINOLate)_3La$ (**1-La**, 30 mg) was added to a 4 mL vial and dissolved in pyridine (1.0 mL). This vial was then placed within a 20 mL screw-capped vial that was half-filled with dry pentane. After several days of pentane diffusion at room temperature, pale crystals formed that were suitable for X-ray structure determination: ^{1}H NMR (500 MHz, THF-d_8, 25 °C, TMS) $\delta = 6.79$ (m, 4H), 6.89 (m, 2H), 6.98 (d, J(H,H) = 8.7 Hz, 2H), 7.22 (m, 7H), 7.58 (d, J(H,H) = 8.8 Hz, 2H), 7.60 (d, J(H,H) = 8.0 Hz, 2H), 7.65 (m, 3H), 8.52 (m, 7H) ppm; ^{13}C{^{1}H} NMR (125 MHz, THF-d_8) $\delta =$ 119.1, 120.4, 124.4, 124.8, 126.8, 126.9, 128.1, 128.4, 128.5, 136.4, 136.7, 150.9, and 163.5 ppm. Anal. Calcd for $C_{95}H_{71}Li_3O_6N_7La$: C, 72.85; H, 4.57; N, 6.26; Found: C, 72.98; H, 4.78; N, 6.12.[34]

4.3.2. Crystallization of $Li_3(py)_5(BINOLate)_3Yb(py)$ (4-Yb). The synthesis of **4-Yb** was obtained by room-temperature diffusion of pentane into a pyridine (1.0 mL) solution of $Li_3(THF)_3$-$(BINOLate)_3Yb$ (**1-Yb**, 0.108 mg) under anhydrous conditions. After several days, pale crystals formed that were suitable for an X-ray diffraction study: ^{1}H NMR (300 MHz, THF-d_8, 25 °C, TMS) $\delta = 7.60$ (br s, 16H, py), 7.93 (t, J(H,H) = 7.4 Hz, 8H, py), 9.31 (br s, 16H, py), -13.22 (br s, 6H), -1.05 (br s, 6H), 2.84 (br s, 6H), 8.08 (d, J(H,H) = 7.89 Hz, 6H), 23.00 (br s, 6H), 85.04 (br s, 6H) ppm; ^{13}C{^{1}H} NMR (75 MHz, THF-d_8) $\delta = 58.1$, 108.2, 110.8, 114.1, 116.2, 121.4, 123.9, 124.4, 125.2, 137.1, 139.8, 152.4, and 177.3 ppm. Anal. Calcd for $C_{90}H_{66}Li_3O_6N_6Yb \cdot 2py$: C, 71.51; H, 4.56; N, 6.67; Found: C, 71.18; H, 4.49; N, 6.75.[35]

4.3.3. Crystallization of $Li_3(py)_5(BINOLate)_3Eu(py)$ (4-Eu). $Li_3(THF)_3(BINOLate)_3Eu$ (**1-Eu**, 0.108 g) was added to a vial and dissolved in 1.0 mL of pyridine. This vial was then placed inside of a 20 mL screw-capped vial that was half-filled with dry pentane. After several days, yellow crystals formed that were suitable for an X-ray diffraction study.

4.4. General Procedure C: Synthesis of $Li_3(DMEDA)_3$-$(BINOLate)_3Ln$ (5-Ln) Complexes from $Ln(O_3SCF_3)_3$. 4.4.1. Synthesis of $Li_3(DMEDA)_3(BINOLate)_3La$ (5-La). Li_2(*R*-BINOLate) (0.763 g, 2.56 mmol) was dissolved in 60 mL of THF, and $La(O_3SCF_3)_3$ (0.500 g, 0.853 mmol) was added as a solid to this clear solution. After 30 min, $La(O_3SCF_3)_3$ completely dissolved, and the cloudy solution once again became clear. This mixture stirred for an additional hour, and DMEDA (0.300 mL, 0.248 g, 2.82 mmol) was added. The clear solution was stirred for a total of 3 days and filtered through dried Celite, the filtrate was recovered, and the volatiles were removed under reduced pressure. The remaining solid was dissolved in CH_2Cl_2, the insoluble materials were removed by filtration through Celite, and the filtrate was collected. The solvent was then removed under reduced pressure to yield a white solid. Washing this solid with diethyl ether and drying it under reduced pressure gave 0.790 g of **5-La** [73% yield based on $La(O_3SCF_3)_3$]. Crystals of **5-La** were obtained by slow diffusion of pentane into a THF solution containing this compound at room temperature: ^{1}H NMR (300 MHz, THF-d_8, 25 °C, TMS) $\delta = 0.61$ (br s, 2H, NH), 1.60 (s, 6H, N-CH_3), 1.69 (br d, 2H, N-CH_2), 1.96 (br d, 2H, N-CH_2), 6.83 (d, 2H), 6.91 (m, 4H), 7.23 (d, 2H), and 7.67 (t, 4H) ppm; ^{13}C{^{1}H} NMR (75 MHz, THF-d_8) $\delta = 36.1$ (N-CH_3), 50.7 (N-CH_2), 119.4, 120.4, 125.0, 126.1, 127.2, 127.9, 128.2, 128.6, 136.6, and 163.8; IR (KBr) $\nu = 3341$, 3299, 3043, 2981,2952, 2890, 2855, 2802, 1612, 1588, 1553, 1499, 1463, 1422, 1342, 1283, 1247, 1177, 1140, 1096, 1069, 994, 959, 935, 882, 822, 746, 665, 632, 591, 574 cm^{-1}. Anal. Calcd for $C_{72}H_{72}Li_3O_6N_6La$: C, 67.71; H, 5.68; N, 6.58. Found: C, 67.35; H, 5.67; N, 6.30.[34]

4.4.2. Synthesis of $Li_3(DMEDA)_3(BINOLate)_3Eu$ (5-Eu) from $Eu(O_3SCF_3)_3$. General procedure C was followed to prepare **5-Eu**. The reagents used are as follows: Li_2(*R*-BINOLate) (0.745 g, 2.50 mmol), $Eu(O_3SCF_3)_3$ (0.500 g, 0.834 mmol), and DMEDA (0.295 mL, 0.244 g, 2.77 mmol) in 60 mL of THF. Compound **5-Eu** (0.650 g) was obtained as a yellow solid in 61% yield based on $Eu(O_3SCF_3)_3$. Crystals of **5-Eu** can be obtained by slow diffusion of pentane into a THF solution containing this compound at room temperature: ^{1}H NMR (300 MHz, THF-d_8, 25 °C, TMS) $\delta = -9.16$ (br s, 2H, NH), -3.82 (br s, 2H, N-CH_2), -3.59 (br s, 2H, N-CH_2), 0.366 (s, 6H, N-CH_3), -1.69 (d, 2H), 3.04 (t, 2H), 5.56 (t, 2H), 7.65 (d, 2H), 13.76 (br s, 2H), 40.56 (br s, 2H) ppm; ^{13}C{^{1}H} NMR (75 MHz, THF-d_8) $\delta = 33.2$ (N-CH_3), 43.8 (N-CH_2), 86.0, 116.4, 116.9, 122.1, 122.6, 128.6, 130.5, 132.4, 134.5, and 180.4 ppm; IR (KBr) $\nu = 3342$, 3299, 3043, 2985, 2952, 2875, 2856, 2803, 1612, 1589, 1554, 1501, 1463, 1423, 1342, 1283, 1248, 1175, 1138, 1096, 1069, 995, 959, 935, 898, 821, 746, 665, 642, 591, 574 cm^{-1}. Anal. Calcd for $C_{72}H_{72}Li_3O_6N_6Eu \cdot THF$: C, 67.01; H, 5.92; N, 6.17. Found: C, 67.26; H, 6.35; N, 5.99.[34]

4.4.3. Synthesis of $Li_3(DMEDA)_3(BINOLate)_3Lu$ (5-Lu) from $Lu(O_3SCF_3)_3$. General procedure C was followed to prepare **5-Lu**. The reagents used are as follows: Li_2(*R*-BINOLate) (0.719 g, 2.41 mmol), $Lu(O_3SCF_3)_3$ (0.500 g, 0.804 mmol), and DMEDA (0.285 mL, 0.234 g, 2.65 mmol) in 60 mL of THF. Compound **5-Lu** (0.665 g) was obtained as a white solid in 63% yield based on $Lu(O_3SCF_3)_3$. Crystals of **5-Lu** were obtained by slow diffusion of pentane into a THF solution containing this compound at room temperature: ^{1}H NMR (300 MHz, THF-d_8, 25 °C, TMS) $\delta = -0.54$ (br s, 2H, N−H), 1.46 (br d, 2H, N-CH_2), 1.63 (s, 6H, N-CH_3), 1.77 (br d, 2H, N-CH_2), 6.87 (br-d, $J = 3.65$, 12H), 6.95 (m, 6H), 7.39 (d, $J = 8.73$, 6H), 7.69 (d, $J = 7.98$, 6H), 7.77 (d, $J = 8.82$, 6H) ppm; ^{13}C{^{1}H} NMR (75 MHz, THF-d_8) δ 36.2 (N-CH_3), 50.2 (N-CH_2), 119.1, 121.2, 125.5, 126.0, 127.1, 128.5, 128.6, 128.6, 136.3, and 163.0 ppm.

4.4.4. Synthesis of $Li_3(DMEDA)_3(BINOLate)_3Y$ (5-Y) from $Y(O_3SCF_3)_3$. General procedure C was followed to prepare **5-Y**. The reagents used are as follows: Li_2(*R*-BINOLate) (0.834 g, 2.80 mmol), $Y(O_3SCF_3)_3$ (0.500 g, 0.933 mmol), and DMEDA (0.331 mL, 0.271 g, 3.08 mmol) in 60 mL of THF. Compound **5-Y** (0.772 g) was obtained as a white solid in 67% yield based on $Y(O_3SCF_3)_3$. Crystals of **5-Y** were obtained by slow diffusion of pentane into a THF solution containing this compound at room temperature: ^{1}H NMR (300 MHz, THF-d_8, 25 °C, TMS) $\delta = -0.29$ (br s, 2H, N−H), 1.61 (br d, 2H, N-CH_2), 1.70 (s, 6H, N-CH_3), 1.89 (br d,

2H, N-CH_2), 6.87 (br-d, J = 3.78, 12H), 6.97 (m, 6H), 7.33 (d, J = 8.76, 6H), 7.69 (d, J = 7.98, 6H), 7.76 (d, J = 8.79, 6H) ppm; $^{13}C\{^1H\}$ NMR (75 MHz, THF-d_8) δ 36.2 (N-CH_3), 50.5 (N-CH_2), 119.1, 121.1, 125.5, 126.0, 126.9, 128.5, 128.6, 136.3, and 162.9 ppm.

4.5. General Procedure D: Synthesis of Li_3(DMEDA)$_3$(BINOLate)$_3$Ln (5-Ln) from Li_3(THF)$_3$(BINOLate)$_3$Ln (1-Ln) Complexes. 4.5.1. Synthesis of Li_3(DMEDA)$_3$(BINOLate)$_3$La (5-La). Li_3(THF)$_3$(BINOLate)$_3$La (**1-La**) (0.500 g, 0.407 mmol) was dissolved in THF (40 mL), and DMEDA (0.143 mL, 0.118 g, 1.34 mmol) was added to this solution. This solution was stirred at room temperature under nitrogen for 4 h, after which all volatile materials were removed in vacuo. The remaining white solid was placed on a frit and washed with diethyl ether (3 × 5 mL) to afford **5-La** after drying under reduced pressure (0.470 g, 91% yield based on **1-La**). The NMR data for this compound were identical to those outlined above.

4.5.2. Synthesis of Li_3(DMEDA)$_3$(BINOLate)$_3$Eu (5-Eu) from Li_3(THF)$_3$(BINOLate)$_3$Eu (1-Eu). General procedure D was followed to prepare **5-Eu**. The synthesis of **5-Eu** was achieved by addition of DMEDA (0.141 mL, 0.117 g, 1.33 mmol) to Li_3(THF)$_3$(BINOLate)$_3$Eu (**1-Eu**) (0.500 g, 0.403 mmol) in THF (40 mL), yielding 0.440 g of product [85% yield based on **1-Eu**]. The NMR data for this compound were identical to those outlined above.

4.5.3. Synthesis of [Li_6(en)$_6$(BINOLate)$_6$Eu$_2$][μ-η^1,η^1-en] (6-Eu). Under a nitrogen atmosphere, ethylene diamine (0.108 mL, 0.097 g, 1.61 mmol) was added to a 40 mL THF solution of Li_3(THF)$_3$(BINOLate)$_3$Eu (**1-Eu**, 0.500 g, 0.407 mmol). After this solution was stirred at room temperature for 12 h, the volatile materials were removed under reduced pressure. The remaining yellow solid was placed on a frit, washed with hexanes, and dried under reduced pressure to afford 0.465 g of **6-Eu** [93% yield based on Li_3(THF)$_3$(BINOLate)$_3$Eu, **1-Eu**]. X-ray-quality crystals were obtained by combining **1-Eu** (100 mg, 0.0814 mmol) and ethylene diamine (21.6 μL, 19.4 mg, 0.322 mmol) in THF and allowing pentane vapor to diffuse into this solution at room temperature. Pale yellow crystals of [Li_6(en)$_7$(BINOLate)$_6$Eu$_2$][μ-η^1,η^1-en] were obtained after several days: ^1H NMR (300 MHz, THF-d_8, 25 °C, TMS) δ = 5.61 (br s, 14H, N−H), 3.92 (br s, 14H, N−C_2H_4−N), 2.49 (d, J = 10.2 Hz, 6H), 4.75 (t, J = 8.59 Hz, 6H), 6.47 (t, J = 8.41 Hz, 6H), 7.44 (d, J = 9.63 Hz, 6H), 9.74 (br s, 6H), 20.80 (br s, 6H) ppm; $^{13}C\{^1H\}$ NMR (75 MHz, THF-d_8) δ = 49.1 (N−C_2H_4−N), 103.6, 116.9, 119.9, 122.7, 124.3, 124.7, 129.8, 131.7, 136.8, and 175.9 ppm.

4.6. NMR Procedure To Determine LISs of Cyclohexenone, DMF, and Pyridine. The ^1H spectra in these studies were obtained on a Bruker DMX-300 Fourier transform NMR spectrometer at 300 MHz. Mesitylene was used as an internal referencing standard for all experiments, and THF-d_8 was used as solvent. Induced chemical shifts of cyclohexenone, *N*,*N*-dimethylformamide (DMF), and pyridine were obtained by incremental addition of known masses of the solid lanthanide complex to a substrate solution of known concentration. All shift reagents (SR), substrates (Sub), and concentration ratios [SR/Sub] are given in Tables 5 (for cyclohexenone and DMF) and 6 (for pyridine). Each sample was allowed to equilibrate for 15 min before acquisition of NMR data. ^1H and $^{13}C\{^1H\}$ NMR spectra for these binding studies are shown in the Supporting Information.

Acknowledgment. We thank the National Institutes of Health, National Institute of General Medical Sciences (GM058101), for a postdoctoral fellowship to A.J.W. We also thank Prof. Michael McBride (Yale University) for very informative discussions on substrate binding to lanthanide complexes and generation of Figure 8, Dr. Sangrama Sahoo for helpful discussion relating to the 2D NMR experiments, and Luca Salvi and Alice Lurain for helpful suggestions.

Supporting Information Available: Procedures and full characterization of new compounds (PDF, CIF). This material is available free of charge via the Internet at http://pubs.acs.org.

JA7107933